



Turner, J., Resendiz Lara, D., Jurca, T., Schaefer, A., Vance, J., Beckett, L. E., ... Manners, I. (2017). Synthesis, characterisation, and properties of poly(aryl)phosphinoboranes formed via iron-catalysed dehydropolymerisation. *Macromolecular Chemistry and Physics*, [1700120]. <https://doi.org/10.1002/macp.201700120>

Peer reviewed version

License (if available):  
Other

Link to published version (if available):  
[10.1002/macp.201700120](https://doi.org/10.1002/macp.201700120)

[Link to publication record in Explore Bristol Research](#)  
PDF-document

This is the author accepted manuscript (AAM). The final published version (version of record) is available online via Wiley at <http://onlinelibrary.wiley.com/doi/10.1002/macp.201700120/abstract>. Please refer to any applicable terms of use of the publisher

## University of Bristol - Explore Bristol Research

### General rights

This document is made available in accordance with publisher policies. Please cite only the published version using the reference above. Full terms of use are available:  
<http://www.bristol.ac.uk/pure/about/ebr-terms>

## Full Paper

# Synthesis, Characterisation, and Properties of Poly(aryl)phosphinoboranes Formed *via* Iron-catalysed Dehydropolymerisation

Joshua R. Turner, Diego A. Resendiz-Lara, Titel Jurca, André Schäfer, James R. Vance, Laura Beckett, George R. Whittell, Rebecca A. Musgrave, Hazel A. Sparkes and Ian Manners\*

School of Chemistry, University of Bristol, Cantock's Close, Bristol BS8 1TS, UK.

**Abstract:** The dehydropolymerisation of the primary phosphine-boranes,  $\text{RPH}_2\text{•BH}_3$  (**1a-f**) ( $\text{R} = (3,4\text{-OCH}_2\text{O})\text{C}_6\text{H}_3$  (**a**),  $\text{Ph}$  (**b**), ( $p\text{-OCF}_3$ ) $\text{C}_6\text{H}_4$  (**c**),  $(3,5\text{-CF}_3)_2\text{C}_6\text{H}_3$  (**d**),  $(2,4,6\text{-CH}_3)_3\text{C}_6\text{H}_2$  (**e**),  $(2,4,6\text{-tBu})_3\text{C}_6\text{H}_2$  (**f**)) was explored using the precatalyst  $[\text{CpFe}(\text{CO})_2\text{OTf}]$  (**I**) ( $\text{OTf} = \text{OS}(\text{O})_2\text{CF}_3$ ), based on the earth abundant element Fe. Formation of polyphosphinoboranes  $[\text{RPH-BH}_2]_n$  (**2a-e**) was confirmed by multinuclear NMR spectroscopy, but no conversion of **1f** to **2f** was detected. Analysis by electrospray ionisation mass spectrometry (ESI-MS) confirmed the presence of the anticipated polymer repeat units for **2a-e**. Gel permeation chromatography (GPC) confirmed the polymeric nature of **2a-e** and indicated number-average molecular weights ( $M_n$ ) of 12,000 – 209,000 Da and polydispersity indices (PDI) between 1.14 – 2.17. In contrast, thermal dehydropolymerisation of **1a-e** in the absence of added precatalyst led to formation of oligomeric material. Interestingly, polyphosphinoboranes **2c** and **2d** displayed GPC behaviour typical of polyelectrolytes, with a hydrodynamic radius dependant on concentration. The thermal transition behaviour, thermal stability, and surface properties of thin films were also studied.

## 1. Introduction

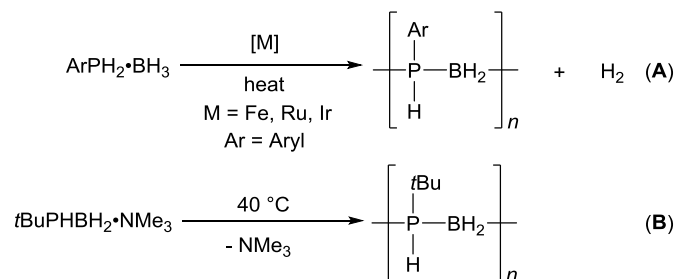
Macromolecules based on main group elements other than carbon, have been the subject of growing interest over the past two decades.<sup>1-3</sup> Current routes to such species are typically based on polycondensation, ring-opening polymerisation and metal-catalysed pathways,<sup>4</sup> which have been successfully exploited to access a broad range of main group polymers; selected examples include polyphosphazenes  $[\text{R}_2\text{PN}]_n$  and related materials,<sup>1,5</sup> polysiloxanes  $[\text{R}_2\text{SiO}]_n$ ,<sup>1,6</sup> polysilanes  $[\text{SiR}_2]_n$ ,<sup>1,7</sup> polystannanes  $[\text{SnR}_2]_n$  ( $\text{R} = \text{alkyl}$ ),<sup>8</sup> boron-nitrogen polymers such as polyaminoboranes  $[\text{NRH-BH}_2]_n$

(R = alkyl, or H),<sup>9</sup> and their congener polyphosphinoboranes [PRH–BH<sub>2</sub>]<sub>n</sub> (R = aryl).<sup>10</sup> The desirable properties of these materials has facilitated a broad range of applications such as elastomers, biomaterials, polyelectrolytes, ceramic precursors, lithographic resists and in optoelectronics.<sup>1-11</sup> Through the use of metal-catalysed dehydrocoupling routes, an increasing number of main group polymers have been synthesised.<sup>2,4b</sup>

As polyphosphinoboranes and polyaminoboranes possess main-chains formed of alternating group 13 and 15 elements, they are formally isoelectronic to those based on C–C main chains. This facet has historically aroused fundamental curiosity in such materials.<sup>12</sup> Moreover, polyphosphinoboranes attracted initial interest in the 1950's, when it was postulated that these materials would have high thermal stability and potential flame retardant properties.<sup>13,14</sup> Primary and secondary phosphine-borane adducts (Me<sub>2</sub>PH•BH<sub>3</sub>, MePH<sub>2</sub>•BH<sub>3</sub>) were thermally dehydrocoupled at ca. 200 °C and above. Despite several instances of reports alluding to formation of polymeric materials in low yield, these products were not convincingly structurally characterized by present day standards, and their macromolecular nature was not established.<sup>14-16</sup>

Over a decade ago, our group reported the first example of metal-catalysed dehydropolymerisation of primary phosphine-boranes.<sup>10a</sup> This process was promoted by an apparently homogenous mechanism, using Rh based precatalysts, [Rh(1,5-COD)Cl]<sub>2</sub> (COD = Cyclooctadiene) and [Rh(1,5-COD)<sub>2</sub>][OTf] (OTf = [OS(O)<sub>2</sub>CF<sub>3</sub>]<sup>-</sup>), operating under melt conditions at temperatures of ca. 130 °C (**Scheme 1A**).<sup>10a,10b,10d,10g</sup> Soluble polymeric material of high molecular weight ( $M_n > 10,000$  Da) was synthesised, but this method also produced crosslinked, swellable, and insoluble material.<sup>10a</sup> Similar catalyst systems have been used to synthesise other polyphosphinoboranes, and demonstrate selective cross-dehydrocoupling with no evidence for P–P or B–B homocoupling.<sup>10h,17</sup> Furthermore, work has been performed to elucidate a mechanism through experimental work with Rh catalysts.<sup>18,19</sup> Recently, the precatalyst [(*t*BuPOCOP)IrH<sub>2</sub>] (*t*BuPOCOP =  $\kappa^3$ -C<sub>6</sub>H<sub>3</sub>-1,3-(OP*t*Bu<sub>2</sub>)<sub>2</sub>) has also been shown to dehydropolymerise primary phosphine-boranes (RPH<sub>2</sub>•BH<sub>3</sub>) (R = Ph, *p*Tol, Mes) in solution at 100 °C.<sup>10k</sup> Furthermore, a metal-free thermolysis based route has been developed for the polymerisation of Lewis based-stabilised phosphinoboranes leading to poly(alkylphosphinoboranes) with appreciable

molecular weight (28,000 – 35,000 Da, PDI < 2) (**Scheme 1B**).<sup>10j,20</sup> This metal-free thermolysis route represents an advancement in the field, as the synthesis of high molecular weight poly(alkylphosphinoboranes) by metal catalysed routes has not been reported.<sup>10d</sup>



**Scheme 1.** Typical methods of synthesising primary polyphosphinoboranes by transition metal catalysed dehydrocoupling (**A**) or via transient formation of phosphinoboranes (**B**).

In 2015, our group reported the use of the iron precatalyst  $[\text{CpFe}(\text{CO})_2\text{OTf}]$  (**I**) as a dehydropolymerisation precatalyst to synthesise polyphosphinoboranes with high molar mass, thereby circumventing the use of rare/expensive transition metals.<sup>10i</sup> Unlike previous systems, the homogenous Fe-based catalytic process yielded high molecular weight poly(phenylphosphinoborane), with polydispersities that were lower than previous reports in the field. This was also achieved with the added advantage of operating under relatively mild conditions (100 °C), and in solution rather than a solvent-free melt. Some degree of control over the molecular weight of the polymer was enabled by changing catalyst loading, such that a lower catalyst loading resulted in higher molecular weights. Furthermore, at low conversion high molecular weight polymer was detected which was indicative of a chain growth polymerisation process. Herein we extend on our initial work and describe the dehydropolymerisation of a range of primary phosphine-borane substrates, catalysed by precatalyst **I**. The goal was to expand the potential scope of this Fe catalyst to demonstrate its utility in preparing high molecular weight polyphosphinoborane polymers with different properties resulting from the variation of pendant organic groups at phosphorus.

## 2. Results and Discussion

### 2.1. Synthesis and characterisation of primary phosphine-borane adducts

We targeted the synthesis of a range of sterically and electronically varied phosphine-borane monomers,  $\text{RPH}_2\cdot\text{BH}_3$  (**1a-f**) (**Figure 1**), of which **1a** and **1c** and **1d** are reported for the first time herein.<sup>10i</sup>

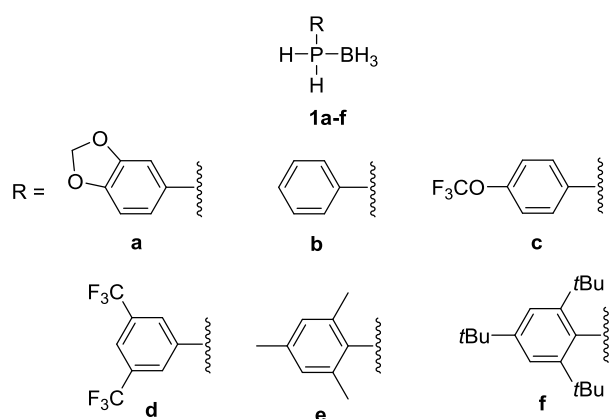
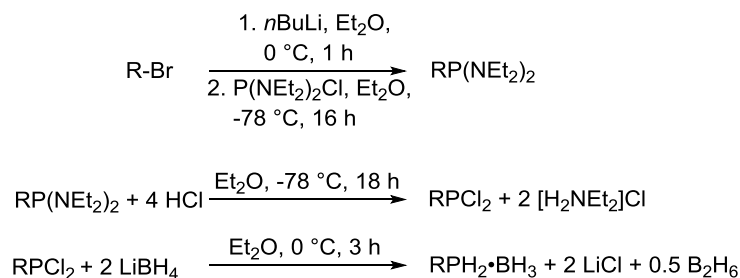


**Figure 1.** Phosphine-borane monomers **1a-f**.

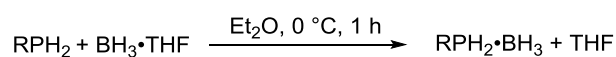
Monomers **1a-f** were isolated in good yield 60 – 70% by two established literature methods. Adducts, **1a**, **1c**, **1d** and **1f** were synthesised by a procedure previously reported by our group,<sup>10g</sup> involving 3 steps starting from the reaction between a protected phosphine  $\text{CIP}(\text{NEt}_2)_2$  and an *in situ* generated organo-lithium reagent  $\text{LiR}$  ( $\text{R} = \text{a, c, d, f}$ ) to form  $\text{RP}(\text{NEt}_2)_2$ . The product was subsequently deprotected and reacted with  $\text{Li}[\text{BH}_4]$  to give phosphine-borane adducts **1a**, **1c**, **1d** and **1f**. The remaining adducts **1b** and **1e** were isolated from the reaction between commercially available primary phosphines  $\text{RPH}_2$  and  $\text{BH}_3\cdot\text{THF}$  (**Scheme 2**). The resulting monomers were characterised by NMR spectroscopy, which afforded spectra consistent with the assigned structures (**Table S1**). For example the  $^{31}\text{P}$  NMR spectrum of **1a** consists of a broad triplet at -46.3 ppm, and a doublet of quartets at -43.5 ppm was observed by  $^{11}\text{B}$  NMR. In the case of **1e** and **1f**, where substitution on the aromatic ring was present in the *ortho*- position, the  $^{31}\text{P}$  and  $^{11}\text{B}$  NMR signals were shifted to higher and lower fields respectively. By  $^1\text{H}$  NMR spectroscopy, the chemical shifts for the P–H protons revealed a trend

whereby the more electron-withdrawing the aromatic ring, according to its corresponding Hammett parameter, the lower the chemical shift of the P–H resonance (**Table S1**).<sup>21</sup>

**Method 1: 1a, 1c, 1d, 1f**



**Method 2: 1b, 1e**



**Scheme 2.** Synthesis of phosphine-borane monomers **1a-f**. Method 1 was used to synthesise **1a**, **1c**, **1d** and **1f**. Method 2 was used to synthesise **1b** and **1e**.

Single, colourless crystals suitable for X-ray analysis were obtained for **1a** and **1c-e** by layering a THF solution with either hexanes or pentane at -40 °C. As expected, the structures of **1a**, and **1c-e** contained tetrahedral phosphorus and boron centres, with similar P–B bond lengths (**1a** 1.922(4) Å, **1c** 1.914(8) Å, **1d** 1.920(5) Å and **1e** 1.925(3) Å) within the range typical for P–B single bonds (1.90 – 2.00 Å) (**Figure 2**).<sup>22</sup>

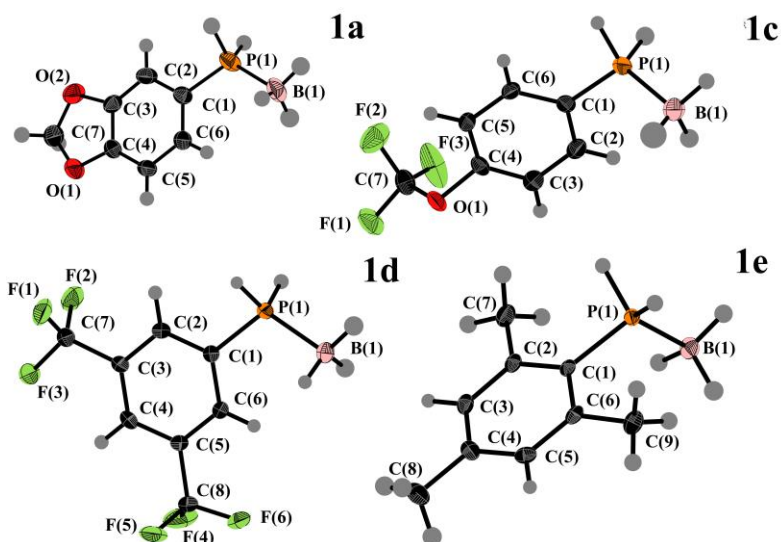


**Figure 2.** Molecular structures for **1a**, **1c**, **1d** and **1e** (thermal ellipsoids set at the 50% probability level). Selected bond distances (Å): **1a**: B(1)–P(1) 1.922(4); **1c**: B(1)–P(1) 1.914(8); **1d**: B(1)–P(1) 1.920(5); **1e**: B(1)–P(1) 1.925(3).

Interestingly, close intermolecular contacts were found in the structures of **1a**, **1c** and **1d**. The structure of **1a** contained  $\pi$ - $\pi$  interactions between pairs of molecules, and in addition a short contact (P(1)–H(1B)···O(1) 2.82(3) Å) was identified (**Figure S1**). The monomer, **1c** crystallised with two molecules in the asymmetric unit ( $z' = 2$ ) and  $\pi$ - $\pi$  stacking interactions were identified between the aryl rings creating staggered stacks approximately along the a-axis direction (**Table S4**). Short intermolecular P–H···H–B contacts were found in **1c**, with distances less than the sum of van der Waals radii of two hydrogen atoms (2.4 Å) (**Figure 3**). Furthermore, one P–H bond was found to be in short contact with an oxygen atom (P(2)–H(2B)···O(2), H(2B)···O(2) 2.58(6) Å), which is within the range of a weak electrostatic hydrogen bond interaction (2.2 – 3.2 Å) (**Figure S2**).<sup>23</sup> These close O···H contacts found in **1a** and **1c** reflect the protic nature of P–H hydrogen. The solid state structure of **1d** was also found to contain intermolecular P–H···H–B contacts of 2.42(6) and 2.52(8) Å, close to the sum of the Van der Waals radii of two H atoms (**Figure S3**). In all the instances of short P–H···H–B intermolecular contacts in **1c** and **1d**, the B–H···H angle (100 – 148°, average: 117°) is smaller relative to the P–H···H angle (118 – 167°, average: 139°), which is consistent to previous reports involving phosphine-boranes and the more thoroughly studied amine-boranes.<sup>24</sup> In the related

$\text{H}_3\text{N}\cdot\text{BH}_3$ , the non-linear  $\text{N}-\text{H}\cdots\text{H}-\text{B}$  interaction was attributed to charge distribution, such that unfavourable dipole interactions are minimised.<sup>25</sup>

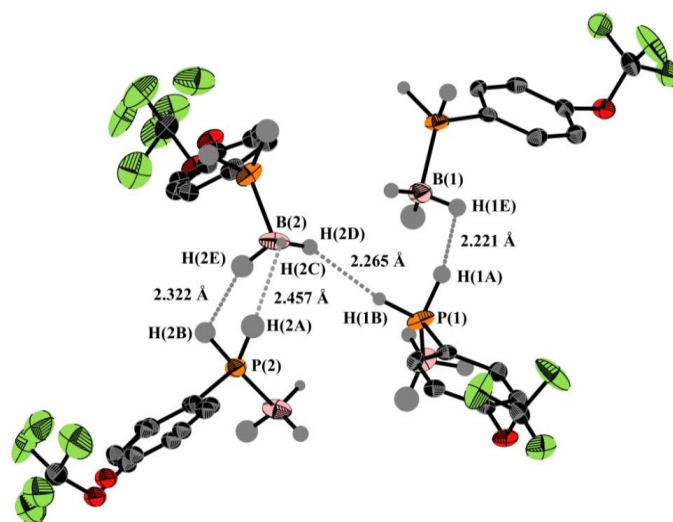


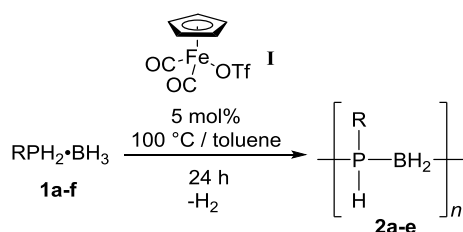
**Figure 3.** Intermolecular  $\text{P}-\text{H}\cdots\text{H}-\text{B}$  solid state contacts between units of **1c**. H atoms on Ph rings have been omitted for clarity and thermal ellipsoids set at the 50% probability level. Selected intermolecular interaction bond lengths (Å) and angles ( $^\circ$ ):  $\text{H}(1\text{E})\cdots\text{H}(1\text{A})$  2.22(9),  $\text{H}(1\text{B})\cdots\text{H}(2\text{D})$  2.27(7),  $\text{H}(2\text{C})\cdots\text{H}(2\text{A})$  2.46(7),  $\text{H}(2\text{E})\cdots\text{H}(2\text{B})$  2.3(1),  $\text{P}(1)-\text{H}(1\text{B})\cdots\text{H}(2\text{D})$  167(4),  $\text{P}(1)-\text{H}(1\text{A})\cdots\text{H}(1\text{E})$  144(4),  $\text{P}(2)-\text{H}(2\text{B})\cdots\text{H}(2\text{E})$  118(4),  $\text{P}(2)-\text{H}(2\text{A})\cdots\text{H}(2\text{C})$  129(3),  $\text{B}(2)-\text{H}(2\text{E})\cdots\text{H}(2\text{B})$  126(5),  $\text{B}(2)-\text{H}(2\text{C})\cdots\text{H}(2\text{A})$  112(3),  $\text{B}(2)-\text{H}(2\text{D})\cdots\text{H}(1\text{B})$  148(5),  $\text{B}(1)-\text{H}(1\text{E})\cdots\text{H}(1\text{A})$  109(4).

In contrast to **1a**, **1c** and **1d**, no analogous intermolecular contacts could be found in the structure of **1e**, which we attribute to the increased steric congestion imposed by the mesityl group. This is supported by the report that the primary alkyl phosphine-borane menthyl $\text{PH}_2\cdot\text{BH}_3$ , does contain short  $\text{P}-\text{B}$  contacts, with the corresponding  $\text{H}\cdots\text{H}$  distances between two monomer units between 2.6 and 2.7 Å.<sup>26</sup> This suggests that intermolecular interactions are still present even for phosphine-boranes with a  $\text{P}-\text{H}$  bond of lower acidity. No intermolecular  $\text{B}-\text{H}\cdots\text{H}-\text{P}$  contacts could be found for crystallographically characterised secondary phosphine-boranes, such as  $\text{Mes}_2\text{PH}\cdot\text{BH}_3$  and  $(p\text{-CF}_3\text{C}_6\text{H}_4)_2\text{PH}\cdot\text{BH}_3$ .<sup>10g,27</sup> These examples suggest that the steric demands of the R group induces the molecules to adopt a solid state structure such that no  $\text{P}-\text{H}\cdots\text{H}-\text{B}$  contacts can form. This would explain that whilst **1e** contains a  $\text{P}-\text{H}$  bond of higher polarity than menthyl $\text{PH}_2\cdot\text{BH}_3$ , the steric demands of the mesityl groups dictate the conformation and packing.



## 2.2. Iron-catalysed dehydrocoupling of the primary phosphine-borane adducts, RPH<sub>2</sub>•BH<sub>3</sub>: Polymer synthesis and characterisation

The newly prepared polymers, **2a** and **2c-e** were synthesised under identical conditions to the previously reported Fe-catalysed formation of **2b**.<sup>10i</sup> This involved heating toluene solutions of RPH<sub>2</sub>•BH<sub>3</sub> (R = **a-f**), and 5 mol% **I** at 100 °C for 24 h under N<sub>2</sub> (**Scheme 3**). Consistent with previous work, a colour change from red to yellow was observed within 5 min. of heating, consistent with the formation of the intermediate [CpFe(CO)<sub>2</sub>(PRH•BH<sub>3</sub>)] (R = **a-f**).<sup>10i</sup> After 24 h, complete consumption of monomer and subsequent formation of polyphosphinoborane, [RPH–BH<sub>2</sub>]<sub>n</sub> (**2a-e**) was confirmed by *in situ* <sup>11</sup>B and <sup>31</sup>P NMR spectroscopy. Monomer **1f** did not undergo dehydrocoupling to form **2f**.

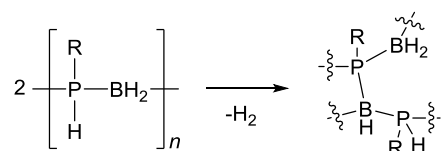


**Scheme 3.** Typical dehydrocoupling reaction for the dehydropolymerisation of monomers **1a-f** to form the polyphosphinoboranes **2a-e** (**2d** was formed using 2 mol% **I**).

Polymers **2c** and **2d**, featuring fluorinated substituents, were purified by precipitation from Et<sub>2</sub>O into cold (-78 °C) pentane, whilst **2a** and **2e** were purified by dissolution in minimal THF and precipitation into pentane at -78 °C.<sup>10i</sup> The polymers obtained were pale yellow/off white solids, where the pale yellow colour likely originates from residual Fe species (**Figure S5, S9, S13, S17**). Polymers **2a-e**, could be handled in air, consistent with previous reports on **2b** and **2e** prepared using precious metal precatalysts.<sup>10i,10k</sup> Further precipitation steps led to a decrease in the intensity of the yellow colour, however these extra steps reduced the isolated yield of the polymer. Complete removal of encapsulated solvent from the polymers was found to be a challenge, typically requiring heating of the sample (40 °C) in *vacuo* for several days. To aid in the removal of residual solvent, which was typically THF or toluene, the polymers could be dissolved in a minimal amount of dichloromethane, and reprecipitated into cold pentane (-78 °C). In the case of **2d**, heating the sample to 60 °C in *vacuo*

for several days was required to completely remove encapsulated solvent, otherwise ca. 10 wt% toluene remained, as detected by TGA. Upon drying, the polymers displayed a slower dissolution rate, typically requiring vigorous stirring for redissolution in either dichloromethane or THF.

At a catalyst loading of 5 mol% of **I**, the dehydropolymerisation of **1d** after 24 h of heating at 100 °C in toluene led to formation of a precipitate. This gummy insoluble solid swelled upon solvent addition, consistent with a non-negligible degree of crosslinking (**Scheme 4**). The supernatant was separated from the gel, concentrated and added to cold pentane (-78 °C) which caused a yellow solid to precipitate in 10% yield. A sample of the solid was analysed by GPC and was found contain polymeric material ( $M_n = 77,000$ , PDI = 1.35) (**Figure S23**). By reducing the catalyst loading to 2 mol%, isolation of a yellow solid, which did not give a gel in chloroform, was possible and in higher yield (31%). The higher yielding material synthesised at 2 mol% catalyst loading was used for all subsequent analysis. The formation of gels was also found for polymers synthesised by Rh methods at high degrees of conversion, where a significant degree of crosslinking was suggested to have taken place.<sup>10b</sup> Polymer **2d** contains the most electron withdrawing substituent at phosphorus and therefore the most activated P–H bond, which increases the likelihood of cross-linking via further H<sub>2</sub> loss leading to formation of gels. In contrast, polymers **2a-c** and **2e** synthesised through the use of precatalyst **I** did not form solvent swellable cross-linked gels in solvents such as chloroform, THF and dichloromethane. These observations suggest an increased linearity for the polymers synthesised using the Fe-precatalyst **I**, compared to those prepared with Rh catalysts under melt conditions, which is consistent with their lower PDI values.<sup>10d</sup>



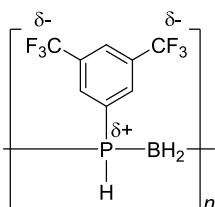
**Scheme 4.** Possible route to crosslinking polyphosphinoborane chains between B and P, enabled by interchain loss of H<sub>2</sub>.

Tolerance of catalyst **I** to sterically demanding substituents on the phosphine-borane monomers was explored by comparing the dehydrocoupling reactions of **1b**, **1e** and **1f**, where increasing steric pressure was introduced at the positions *ortho*- and *para*- to the phosphorus on the aromatic ring. While monomers **1b** and **1e** were successfully converted to polymers **2b** and **2e** respectively, no dehydrocoupling was observed for **1f**. Addition of **1f** to 5 mol% of **I** in toluene and heating to 100 °C led to a colour change from red to yellow after 1 h. Over the course of 22 h, monitoring the reaction by <sup>31</sup>P NMR showed only an increase in the amount of free ((2,4,6-*t*Bu)<sub>3</sub>C<sub>6</sub>H<sub>2</sub>)PH<sub>2</sub> was detected (**Figure S20**).

The <sup>11</sup>B and <sup>31</sup>P NMR chemical shifts for the isolated samples of polymers **2a-e** are summarised in **Table 1**. Consistent with previous reports on polymers **2b** and **2e**, the <sup>11</sup>B NMR chemical shift, found at -35 ppm, was broad due to unresolved coupling to proton for **2a-e**.<sup>10i,10k</sup> The <sup>31</sup>P NMR chemical shift was found between -46 and -49 ppm for **2a-d**, and at -74 ppm for **2e**. The different aromatic groups in **2a-d** did not have an obvious impact on the <sup>11</sup>B and <sup>31</sup>P NMR chemical shifts, except when the polymer contained a substituent in the *ortho*- position (**2e**), but only in the latter case. The expected P–H coupling by <sup>31</sup>P NMR could only be resolved for **2b** (<sup>1</sup>J<sub>PH</sub> = 349 Hz) and **2e** (<sup>1</sup>J<sub>PH</sub> = 350 Hz). Furthermore, the <sup>31</sup>P NMR spectra of **2c** and **2d** contained a peak that resembled a virtual 1:2:1 triplet at 46 – 49 ppm (**Figure S8** and **S12**). This pattern is consistent with the formation of an atactic polymer, with resolution of the triad structure, which was also reported for primary polyphosphinoboranes, [(*p*-CF<sub>3</sub>C<sub>6</sub>H<sub>4</sub>)PH–BH<sub>2</sub>]<sub>*n*</sub> and [*t*BuPH–BH<sub>2</sub>]<sub>*n*</sub>.<sup>10g,10j</sup> This fine structure could not be resolved spectroscopically for **2a**, **2b** or **2e**. Compared with the NMR spectra of the monomers **1a-e**, the <sup>11</sup>B NMR spectra of **2a-e** revealed a downfield shifted resonance. The P–H chemical shift in the <sup>1</sup>H NMR spectrum provided further contrast, where a doublet was found at a higher field than in the monomer. For example, the chemical shift for the PH<sub>2</sub> protons of **1a** was found at 5.47 ppm, whilst a value of 4.39 ppm was found for **2a**.

### 2.3. Molar mass characterisation

Electrospray ionisation mass spectrometry (ESI-MS) was performed on solutions of **2a**, **2c**, **2d** and **2e** in CH<sub>2</sub>Cl<sub>2</sub>. A repeating pattern corresponding with successive loss of [RHP–BH<sub>2</sub>] units, however was only detected up to 2,500 – 4,000 Da (**Figure S29-S32**). The molecular weight of these polymers was also investigated by gel permeation chromatography (GPC), which indicated that the materials were of high molecular weight polymers (**Table 1**). Previous work involving polyphosphinoboranes, analysed by GPC in THF, revealed problems concerning molecular weight characterisation due to facile aggregation and/or adsorption of the polymer chains onto the GPC column solid-phase material.<sup>10d</sup> The problems were resolved through increasing the ionic strength of the eluent through use of [Bu<sub>4</sub>N]Br, which we have previously found effective in reducing column adsorption effects. By studying variations in the concentration of samples it was evident that poly(phenylphosphinoborane) showed no column adsorption.<sup>10d</sup> Thus, for **2a** and **2e** the concentration of the GPC sample also had no effect on the elution volume, and therefore the calculated PDI or molecular weight (**Figure S6 and S18**). However, for the polymers containing fluorinated groups, **2c** and **2d**, a reversible, inverse dependency of elution volume on concentration was observed (**Figure S10 and S14**). This GPC behaviour is reminiscent to that of polyelectrolytes, where the lower concentration causes larger intrachain repulsion, thereby increasing the observed hydrodynamic radius.<sup>28,29</sup> Although, there is no clear explanation at this time, we postulate that the presence of electron-withdrawing substituent on phosphorus enhances the existing polarisation of the P–B backbone and results in a partial negative charge at the polymer periphery (**Scheme 5**).<sup>30</sup>



**Scheme 5.** Schematic representation of electron density for polymers **2c** and **2d**.

Formation of polymer, **2e** has been previously reported by catalytic method based on Ir.<sup>10k</sup> With the [Ir(POCOP)H<sub>2</sub>] catalyst system, at 2.5 mol% catalyst loading, polymeric material (M<sub>n</sub> = 33,000 Da) with a PDI of 1.8 was formed. In the case of **1**, a slightly higher molecular weight (M<sub>n</sub> = 95,000 Da) polymer with a PDI of 1.14 polymer was formed.

Catalyst free, thermal dehydropolymerisation occurred for **1a-e** in solution. Thus, heating samples of **1a-e** in toluene to 100 °C for 24 h under N<sub>2</sub> resulted in incomplete conversion (70 – 90%) and formation of only low molecular weight (M<sub>n</sub> = < 2,300 – 4,500 Da) (**Figure S24-S28**) and polydisperse (PDI = 2.0 – 8.0) material. The metal-catalysed route led to complete consumption of monomer after 24 h leading to formation of a polyphosphinoborane product that had a higher molecular weight and a lower polydispersity. These results suggest that non-metal catalysed reactions can also occur under the conditions used for the metal-catalysed dehydropolymerisation and these may explain the detection of the detected low-molecular weight material for **2a-e**.<sup>9b</sup>

**Table 1.** Summary of <sup>11</sup>B NMR, <sup>31</sup>P NMR (**Figure S4, S8, S12** and **S16**), and GPC results (**Figure S7, S11, S15** and **S19**) for polyphosphinoboranes **2a-e**.

Polymer	<sup>11</sup> B shift <sup>d</sup> (ppm)	<sup>31</sup> P shift <sup>d</sup> (ppm) ( <sup>1</sup> J <sub>PH</sub> (Hz))	M <sub>w</sub> (Da) <sup>c</sup>	M <sub>n</sub> (Da) <sup>c</sup>	PDI	DP <sub>n</sub>
<b>2a</b>	-35	-47 (350)	26,000	12,000	2.17	72
<b>2b</b> <sup>b</sup>	-35	-49 (349)	72,000	45,000	1.60	369
<b>2c</b> <sup>a</sup>	-35	-49 (350)	107,000	79,000	1.35	383
<b>2d</b> <sup>a</sup>	-35	-46 (360)	262,000	209,000	1.25	810
<b>2e</b>	-35	-74 (335)	108,000	95,000	1.14	579

<sup>a</sup>A concentration based effect was observed for GPC results, see main text. <sup>b</sup>ref. 10i. <sup>c</sup>2 mg/mL.

<sup>d</sup>NMR spectroscopy was carried out in CDCl<sub>3</sub>.

#### 2.4. Thermal Transitional Behaviour and Stability of Polymers **2a-e**

The thermal transition behaviour of the polyphosphinoboranes **1a**, **1c**, **1d** and **1e** was investigated by differential scanning calorimetry (DSC) and thermogravimetric analysis (TGA) (**Table 2**). Glass transition temperatures for **2a**, **2c** and **2d** could be determined by DSC, at a scan rate of 10 °C/min (**Figure S33-S35**). The observed glass transition temperature of 82 °C for **2a**, is higher than that previously reported for **2b** (38 °C). This could be due to increased rigidity of the polymer chain,

which is induced by the presence of the -OCH<sub>2</sub>O- substituent. Polymer **2c** was found to have a lower glass transition temperature of 29 °C relative to that of **2b**. The lower glass transition temperature for the former material might be explained by the smaller barrier of rotation for the trifluoromethoxy group which has the effect of introducing chain flexibility into and additional free volume.<sup>31</sup> The T<sub>g</sub> of **2d** (52 °C), higher than **2b** (38 °C), is consistent with the trend detected when comparing the organic polymers polystyrene (105 °C) and poly(2,5-bis(trifluoromethyl)styrene) (116 °C).<sup>32,33</sup> For **2e**, no glass transition was observed below ca. 135 °C, above which decomposition of the polymer occurred. Compared with polystyrene, the glass transition temperature of **2b** is considerably lower. This difference has previously been attributed to the higher degree of torsional flexibility in the polymer main chain as a result of the longer main chain P–B bonds.<sup>10d</sup>

**Table 2.** Summary of the thermal properties, T<sub>g</sub>, T<sub>5%</sub>, and ceramic yield of **2a-e**.

Polymer	R Substituent	T <sub>g</sub> (°C)	T <sub>5%</sub> <sup>e)</sup> (°C)	Ceramic Yield <sup>d)</sup> (%)
<b>2a</b>	(3,4-OCH <sub>2</sub> O)C <sub>6</sub> H <sub>3</sub>	82	210	46
<b>2b</b> <sup>a)</sup>	Ph	38	180	55
<b>2c</b>	( <i>p</i> -OCF <sub>3</sub> )C <sub>6</sub> H <sub>4</sub>	29	170	24
<b>2d</b> <sup>b)</sup>	(3,5-CF <sub>3</sub> ) <sub>2</sub> C <sub>6</sub> H <sub>3</sub>	52	150	20
<b>2e</b>	(2,4,6-CH <sub>3</sub> ) <sub>3</sub> C <sub>6</sub> H <sub>2</sub>	>133	160	21

<sup>a)</sup>Ref. 10i. <sup>b)</sup>Samples contained toluene (<10 wt%). <sup>c)</sup>Temperature at 5% weight loss. <sup>d)</sup>Ceramic yields were measured at 700 °C. <sup>e)</sup>Based on idealised conversion to boron-phosphide, BP.

The thermal stability of **2a-e** was further investigated by TGA under an N<sub>2</sub> atmosphere, at a heating rate of 10 °C/min (**Figure 5**). The onset of weight loss for **2a** occurred at around 160 °C, and material showed a T<sub>5%</sub> (temperature at which the polymer has lost 5% of its original weight) at 210 °C. Minimal weight loss occurred between 230 and 320 °C (< 2 wt%) for **2a**, after which a further 30% of mass was lost until 500 °C. For polymers **2b**, **2c** and **2e** the onset of weight loss occurred around 130 °C, after which the majority of mass was lost up until 500 °C. It has previously been suggested that the low thermal stability of these polymers can be explained by the release of a second equivalent of H<sub>2</sub> leading to further decomposition pathways.<sup>10d</sup> Initial weight loss for **2d** was found to occur ca.140 °C, with the majority of loss occurring up to 500 °C. Samples of polymer **2b** prepared with the Fe precatalyst showed a lower temperature for weight loss (T<sub>5%</sub> = 180 °C) compared to those synthesised

with Rh(ii) mediation ( $T_{5\%} = 240\text{ }^{\circ}\text{C}$ ).<sup>10d</sup> This is a likely consequence of a more branched structure in the latter case which would hinder loss of volatile material.

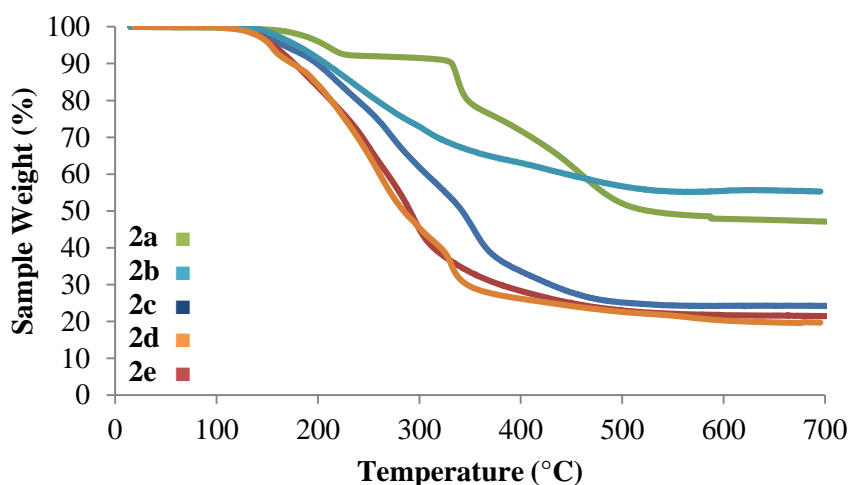


**Figure 5.** TGA thermograms of **2a** (■), **2b** (■), **2c** (■), **2d** (■) and **2e** (■) (heating rate: 10 °C/min).

The ceramic yields after heating to 700 °C were also found to be lower than for previous Rh-based dehydropolymerisation products. Ceramic yields for polymers prepared using a Rh precatalyst were typically in the range of 75 – 80% for aryl polymers and 35 – 45% for polymers containing alkyl substituents at phosphorus.<sup>10d</sup> These are noticeably higher ceramic yields than those found for polymers prepared using Fe-precatalyst **I** (Table 2). This is especially noticeable when comparing the ceramic yield of **2b** between the Rh (75 – 80%) and Fe (55%) catalytic methods.<sup>10d</sup> The lower ceramic yields in this report are consistent with the presence of mainly linear polymeric material since, as noted above, branched polymeric chains hinder the loss of volatile products.

## 2.5. Soft lithography of polyphosphinoboranes and contact angle measurements

To further elaborate on our earlier findings that poly(phenylphosphinoborane) could be patterned on silicon wafers using soft lithography techniques, a similar procedure was used for **2e**; chosen for the large difference in  $T_g$  (> 133 °C) compared to **2b** (35 °C).<sup>10i</sup> The procedure involved drop casting a 2 mg/mL THF solution of **2e** on a clean Si wafer, before patterning using a polydimethylsiloxane stamp at 150 °C for 5 mins. Imaging by scanning electron microscopy revealed excellent retention of shape

and crisp detail along edges (**Figure 6**). However, as anticipated for **2e** on the basis of the higher  $T_g$  compared to **2b**, the resulting material contained noticeably more crack features which are present throughout the sample.

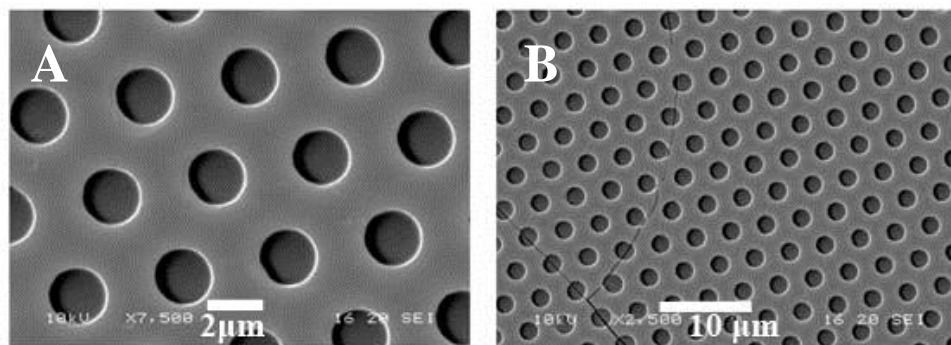


**Figure 6.** Scanning electron microscopy of patterned polymer **2e**, scanning electron micrograms obtained with 2 μm (A) and 10 μm (B) scale bars shown.

Since **2c** and **2d** contain fluorinated groups, we anticipated that thin films of these polymers would display hydrophobic behaviour. Thin films of **2a-e** were formed by spin coating a 5 mg/mL THF solution onto a glass slide, and the advancing water droplet contact angles were subsequently obtained (**Figure 7**). As expected, the contact angles of  $101^\circ$  and  $97^\circ (\pm 2^\circ)$  obtained for **2c** and **2d** suggested a hydrophobic surface. These advancing angles are similar to those found for poly(chlorotrifluoroethylene) ( $99^\circ$ ), but smaller than for the widely used fluorinated polymer, poly(tetrafluoroethylene) (PTFE) ( $109^\circ$ ).<sup>34</sup> Thin films of **2a**, **2b** and **2e** were found to contain hydrophilic surfaces as supported by their advancing contact angles  $64^\circ$ ,  $70^\circ$  and  $78^\circ (\pm 2^\circ)$  respectively. The surfaces of polyphosphinoboranes in general, appear to be more hydrophilic in nature than their organic counterparts, highlighted by comparison between **2b** ( $70^\circ$ ) and the organic analogue polystyrene ( $87^\circ$ ).<sup>35</sup> This is likely to be due to the difference in polarity of the P–H and B–H bonds in the polymer backbone compared with C–H bonds.



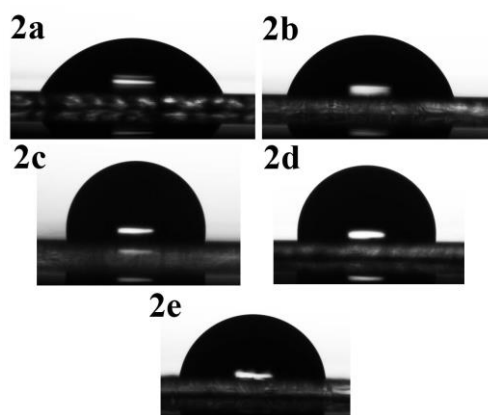


**Figure 7.** Still frames of 2  $\mu\text{L}$  droplets of deionised water deposited on thin films of **2a-e**.

### 3. Summary

The scope of the Fe complex **I** as a precatalyst for the dehydropolymerisation of phosphine-boranes **1a-e** has been explored. Formation of polymers **2a-e**, was achieved in solution at 100 °C in under 24 h in the presence of 5 mol% **I**, however the bulky monomer **1f** was resistant to polymerisation under these conditions. GPC analysis of polymers **2a-e** revealed the formation of high molecular weight polymeric material, and the presence of the expected repeat unit was confirmed by ESI-MS. A concentration dependence in the cases of polymers **2c** and **2d** was detected by GPC analysis. This behaviour is reminiscent of polyelectrolytes and was tentatively attributed to the build up of residual charge on the protruding electronegative organic substituent at phosphorus. Analysis of the thermal properties of polymers **2a-e** revealed glass transition temperatures that were lower than their organic analogues. Furthermore, these materials possessed lower thermal stability compared with polyphosphinoboranes synthesised by previous Rh based methods. Thin film patterning and contact angle measurements indicate that polymer properties are tuneable by altering the substituents at phosphorus. Addition of fluorine containing functional groups, as with the case of organic polymers, had the expected effect of increasing the hydrophobicity of the surface. Ongoing work involves a mechanistic investigation of the dehydropolymerisation process, optimisation of the reaction with a view to scale up and further characterisation of the properties of these polymers. We are also exploring routes to polyphosphinoboranes with non-hydrogen substituents at phosphorus which

should show enhanced thermal stability, and potential behaviour as flame retardant materials will be explored.

## Acknowledgements

The authors would like to acknowledge the Engineering and Physical Sciences Research Council (EPSRC) for financial support.

## References

- [1] Manners, I., *Angew. Chem. Int. Ed.* **1996**, *35* (15), 1602-1621.
- [2] Priegert, A. M.; Rawe, B. W.; Serin, S. C.; Gates, D. P., *Chem. Soc. Rev.* **2016**, *45* (4), 922-953.
- [3] Jäkle, F., *Chem. Rev.* **2010**, *110* (7), 3985-4022.
- [4] (a) Heeney, M.; Zhang, W.; Crouch, D. J.; Chabynyc, M. L.; Gordeyev, S.; Hamilton, R.; Higgins, S. J.; McCulloch, I.; Skabara, P. J.; Sparrowe, D.; Tierney, S., *Chem. Commun.* **2007**, (47), 5061-5063; (b) Leitao, E. M.; Jurca, T.; Manners, I., *Nat. Chem.* **2013**, *5* (10), 817-829; (c) He, G.; Kang, L.; Torres Delgado, W.; Shynkaruk, O.; Ferguson, M. J.; McDonald, R.; Rivard, E., *J. Am. Chem. Soc.* **2013**, *135* (14), 5360-5363; (d) Rawe, B. W.; Gates, D. P., *Angew. Chem. Int. Ed.* **2015**, *54* (39), 11438-11442.
- [5] (a) Allcock, H. R.; Kugel, R. L., *Inorg. Chem.* **1966**, *5* (10), 1716-1718; (b) Neilson, R. H.; Wisian-Neilson, P., *Chem. Rev.* **1988**, *88* (3), 541-562; (c) Liang, M.; Manners, I., *J. Am. Chem. Soc.* **1991**, *113* (10), 4044-4045; (d) Allcock, H. R., *Chem. Mater.* **1994**, *6* (9), 1476-1491; (e) Honeyman, C. H.; Manners, I.; Morrissey, C. T.; Allcock, H. R., *J. Am. Chem. Soc.* **1995**, *117* (26), 7035-7036; (f) Allcock, H. R.; Nelson, J. M.; Reeves, S. D.; Honeyman, C. H.; Manners, I., *Macromolecules* **1997**, *30* (1), 50-56; (g) De Jaeger, R.; Gleria, M., *Prog. Polym. Sci.* **1998**, *23* (2), 179-276; (h) Allcock, H. R., *Soft Matter* **2012**, *8* (29), 7521-7532; (i) Wilfert, S.; Henke, H.; Schoefberger, W.; Brüggemann, O.; Teasdale, I., *Macromol. Rapid Commun.* **2014**, *35* (12), 1135-1141; (j) Allcock, H. R., *Dalton Trans.* **2016**, *45* (5), 1856-1862; (k) Rothmund, S.; Teasdale, I., *Chem. Soc. Rev.* **2016**, *45* (19), 5200-5215; (l) Presa-Soto, D.; Carriedo, G. A.; de la Campa, R.; Presa Soto, A., *Angew. Chem. Int. Ed.* **2016**, *55* (34), 10102-10107.
- [6] (a) Li, Y.; Kawakami, Y., *Macromolecules* **1998**, *31* (17), 5592-5597; (b) Mark, J. E., *Acc. Chem. Res.* **2004**, *37* (12), 946-953.
- [7] (a) West, R., *J. Organomet. Chem.* **1986**, *300* (1-2), 327-346; (b) Miller, R. D.; Michl, J., *Chem. Rev.* **1989**, *89* (6), 1359-1410.
- [8] (a) Imori, T.; Lu, V.; Cai, H.; Tilley, T. D., *J. Am. Chem. Soc.* **1995**, *117* (40), 9931-9940; (b) Trummer, M.; Choffat, F.; Smith, P.; Caseri, W., *Macromol. Rapid Commun.* **2012**, *33* (6-7), 448-460; (c) Harrypersad, S.; Foucher, D., *Chem. Commun.* **2015**, *51* (33), 7120-7123; (d) Caseri, W., *Chem. Soc. Rev.* **2016**, *45* (19), 5187-5199.
- [9] (a) Staubitz, A.; Presa Soto, A.; Manners, I., *Angew. Chem. Int. Ed.* **2008**, *47* (33), 6212-6215; (b) Staubitz, A.; Sloan, M. E.; Robertson, A. P. M.; Friedrich, A.; Schneider, S.; Gates, P. J.; Günne, J. S. a. d.; Manners, I., *J. Am. Chem. Soc.* **2010**, *132* (38), 13332-13345; (c) Vance, J. R.; Robertson, A. P. M.; Lee, K.; Manners, I., *Chem. Eur. J.* **2011**, *17* (15), 4099-4103; (d) Dallanegra, R.; Robertson, A.

P. M.; Chaplin, A. B.; Manners, I.; Weller, A. S., *Chem. Commun.* **2011**, 47 (13), 3763-3765; (e) Marziale, A. N.; Friedrich, A.; Klopsch, I.; Drees, M.; Celinski, V. R.; Schmedt auf der Günne, J.; Schneider, S., *J. Am. Chem. Soc.* **2013**, 135 (36), 13342-13355; (f) Thiedemann, B.; Gliese, P. J.; Hoffmann, J.; Lawrence, P. G.; Sonnichsen, F. D.; Staubitz, A., *Chem. Commun.* **2017**; (g) Wan, W.-M.; Baggett, A. W.; Cheng, F.; Lin, H.; Liu, S.-Y.; Jakle, F., *Chem. Commun.* **2016**, 52 (93), 13616-13619; (h) Lorenz, T.; Lik, A.; Plamper, F. A.; Helten, H., *Angew. Chem. Int. Ed.* **2016**, 55 (25), 7236-7241.

[10] (a) Dorn, H.; Singh, R. A.; Massey, J. A.; Lough, A. J.; Manners, I., *Angew. Chem. Int. Ed.* **1999**, 38 (22), 3321-3323; (b) Dorn, H.; Singh, R. A.; Massey, J. A.; Nelson, J. M.; Jaska, C. A.; Lough, A. J.; Manners, I., *J. Am. Chem. Soc.* **2000**, 122 (28), 6669-6678; (c) Dorn, H.; Vejzovic, E.; Lough, A. J.; Manners, I., *Inorg. Chem.* **2001**, 40 (17), 4327-4331; (d) Dorn, H.; Rodezno, J. M.; Brunnhöfer, B.; Rivard, E.; Massey, J. A.; Manners, I., *Macromolecules* **2003**, 36 (2), 291-297; (e) Denis, J.-M.; Forintos, H.; Szelke, H.; Toupet, L.; Pham, T.-N.; Madec, P.-J.; Gaumont, A.-C., *Chem. Commun.* **2003**, (1), 54-55; (f) Jacquemin, D.; Lambert, C.; Perpète, E. A., *Macromolecules* **2004**, 37 (3), 1009-1015; (g) Clark, T. J.; Rodezno, J. M.; Clendenning, S. B.; Aouba, S.; Brodersen, P. M.; Lough, A. J.; Ruda, H. E.; Manners, I., *Chem. Eur. J.* **2005**, 11 (15), 4526-4534; (h) Pandey, S.; Lönnecke, P.; Hey-Hawkins, E., *Eur. J. Inorg. Chem.* **2014**, 2014 (14), 2456-2465; (i) Schäfer, A.; Jurca, T.; Turner, J.; Vance, J. R.; Lee, K.; Du, V. A.; Haddow, M. F.; Whittell, G. R.; Manners, I., *Angew. Chem. Int. Ed.* **2015**, 54 (16), 4836-4841; (j) Marquardt, C.; Jurca, T.; Schwan, K.-C.; Stauber, A.; Virovets, A. V.; Whittell, G. R.; Manners, I.; Scheer, M., *Angew. Chem. Int. Ed.* **2015**, 54 (46), 13782-13786; (k) Paul, U. S. D.; Braunschweig, H.; Radius, U., *Chem. Commun.* **2016**, 52 (55), 8573-8576.

[11] (a) Clarson, S. J. S., *Siloxane Polymers*. Prentice Hall: Englewood Cliffs, **1993**; (b) Archer, R. D., *Inorganic and Organometallic Polymers*. Wiley-VCH: New York, **2001**; (c) Choffat, F.; Käser, S.; Wolfer, P.; Schmid, D.; Mezzenga, R.; Smith, P.; Caseri, W., *Macromolecules* **2007**, 40 (22), 7878-7889; (d) Rawe, B. W.; Chun, C. P.; Gates, D. P., *Chem. Sci.* **2014**, 5 (12), 4928-4938; (e) Linshoef, J.; Baum, E. J.; Hussain, A.; Gates, P. J.; Näther, C.; Staubitz, A., *Angew. Chem. Int. Ed.* **2014**, 53 (47), 12916-12920; (f) Cao, W.; Gu, Y.; Meineck, M.; Li, T.; Xu, H., *J. Am. Chem. Soc.* **2014**, 136 (13), 5132-5137.

[12] Staubitz, A.; Robertson, A. P. M.; Sloan, M. E.; Manners, I., *Chem. Rev.* **2010**, 110 (7), 4023-4078.

[13] Parshall, G. W., *In The Chemistry of Boron and its Compounds*. Wiley: New York, **1967**.

[14] Burg, A. B.; Wagner, R. I., *J. Am. Chem. Soc.* **1953**, 75 (16), 3872-3877.

[15] Wagner, R. I.; Caserio, F. F., *J. Inorg. Nucl. Chem.* **1959**, 11 (3), 259.

[16] Burg, A. B., *J. Inorg. Nucl. Chem.* **1959**, 11 (3), 258.

[17] Pandey, S.; Lönnecke, P.; Hey-Hawkins, E., *Inorg. Chem.* **2014**, 53 (16), 8242-8249.

[18] Grant, D. J.; Dixon, D. A., *J. Phys. Chem. A* **2006**, 110 (47), 12955-12962.

[19] Hooper, T. N.; Weller, A. S.; Beattie, N. A.; Macgregor, S. A., *Chem. Sci.* **2016**, 7 (3), 2414-2426.

[20] Stauber, A.; Jurca, T.; Marquardt, C.; Fleischmann, M.; Seidl, M.; Whittell, G. R.; Manners, I.; Scheer, M., *Eur. J. Inorg. Chem.* **2016**, (17), 2684-2687.

[21] Hansch, C.; Leo, A.; Taft, R. W., *Chem. Rev.* **1991**, 91 (2), 165-195.

[22] Fox, A.; Hartman, J. S.; Humphries, R. E., *J. Chem. Soc., Dalton Trans.* **1982**, (7), 1275-1283.

- [23] Jeffrey, G. A., *An Introduction to Hydrogen Bonding*. Oxford University Press: **1997**.
- [24] Klooster, W. T.; Koetzle, T. F.; Siegbahn, P. E. M.; Richardson, T. B.; Crabtree, R. H., *J. Am. Chem. Soc.* **1999**, *121* (27), 6337-6343.
- [25] Richardson, T.; de Gala, S.; Crabtree, R. H.; Siegbahn, P. E. M., *J. Am. Chem. Soc.* **1995**, *117* (51), 12875-12876.
- [26] Blank, N. F.; McBroom, K. C.; Glueck, D. S.; Kassel, W. S.; Rheingold, A. L., *Organometallics* **2006**, *25* (7), 1742-1748.
- [27] Pelczar, E. M.; Nytko, E. A.; Zhuravel, M. A.; Smith, J. M.; Glueck, D. S.; Sommer, R.; Incarvito, C. D.; Rheingold, A. L., *Polyhedron* **2002**, *21* (23), 2409-2419.
- [28] Böhme, U.; Scheler, U., *Macromolecular Symposia* **2002**, *184* (1), 349-356.
- [29] Aldebert, P.; Gebel, G.; Loppinet, B.; Nakamura, N., *Polymer* **1995**, *36* (2), 431-434.
- [30] Jacquemin, D.; Perpète, E. A., *J. Phys. Chem. A* **2005**, *109* (28), 6380-6386.
- [31] Shishkov, I. F.; Geise, H. J.; Van Alsenoy, C.; Khristenko, L. V.; Vilkov, L. V.; Senyavian, V. M.; Van der Veken, B.; Herrebout, W.; Lokshin, B. V.; Garkusha, O. G., *J. Mol. Struct.* **2001**, *567-568*, 339-360.
- [32] Rieger, J., *J. Therm. Anal. Calorim.* **1996**, *46* (3-4), 965-972.
- [33] Teng, H.; Lou, L.; Koike, K.; Koike, Y.; Okamoto, Y., *Polymer* **2011**, *52* (4), 949-953.
- [34] S. Wu, *Polymer Interface and Adhesion*, Marcel Dekker, New York, NY, **1982**, p. 142-146.
- [35] Strobel, M.; Thomas, P. A.; Lyons, C. S., *J. Polym. Sci., Part A: Polym. Chem.* **1987**, *25* (12), 3343-3348.

TOC:

